Tuijin Jishu/Journal of Propulsion Technology
ISSN: 1001-4055
Vol. 46 No. 1 (2025)

A Study of Diesel Engine Performance and Emission using Artificial Neural Networks with Biodiesel from used Temple Oil

Anjappa S B[1], D.K Ramesha[2], Shivaranjini[3].

[1,2]Department of Mechanical Engineering, University of Visvesvaraya College of Engineering, Bangaluru-560001, India.

[3]Department of Computer Science and Engineering, Madanapalle Institute of Technology & Science, Madanapalle, andhrapradesh, India..

Abstract: A major threat is environmental pollution, particularly of gases resulting from the combustion of fossil fuels. Transesterification of used temple oil in methyl ester blended biodiesel at 25%, 50%, 75%, and 100% was studied. These were studied to see how they would affect engine emissions and performance. Results at 1500 rpm reduced brake power and thermal efficiency by 25% and 24%, respectively, compared to diesel. Indeed, however, the specific fuel consumption of diesel increased by 23%. According to Cam Bell's analysis, methyl ester blends led to a 15% lower air-fuel ratio and 4% lower volumetric efficiency than diesel. B100 biodiesel showed significant emission reductions: carbon monoxide 12%, hydrocarbons 44%, and smoke 48%. Under full load, NOx emissions were increased by 200 percent. Engine performance and emission modeling were optimized using ANN, leading to a reduction in costs as well as physical effort and facilitating the handling of nonlinear datasets.

Keywords: *Used Temple Oil, Engine Performance and Emission Characteristics, Artificial Neural Network, Multilayer Perceptron Model, Backpropagation Algorithm.*

1. Introduction

The search for alternative fuels for diesel engines has however been necessitated by environmental factors and global depletion of fossile resources . The above challenges can be solved by using biodiesel. Biodiesel as a fuel is different from normal diesel in that it is renewable, biodegradable, non toxic and does not contain sulfur and aromatic [1-3]. But vegetable oils that are directly used in diesel engines suffer from high densities, high viscosity and low volatility which cause bad fuel atomization and spray penetration. This can lead to problems such as engine deposits, high viscosity of the lubricating fluids and unreliable piston ring adhesion [4,5]. The transesterification also increases the quality of the oil especially to be used in the engines. In comparison to standards diesel, biodiesel is associated with lesser amount of emission [5–7]. Further, other research shows that in proportion with the percentage of biodiesel additives in fuel, the characteristics of thermal conductivity and heat dissipation change and thereby leading to low temperature[8,9]. Some literature on biodiesel blends has also indicated that as the biodiesel fraction in the blend rises, then the peak cylinder pressure reduces [10,11]. This is due to the underlying heat release rates in the premixed combustion phase in higher biodiesel blends. Several literatures have been reviewed for assessing the feasibility of a number of pure vegetable oils including fish oil, palm oil, pongamia oil and neem seed oil for biodiesel production [12–14]. A comparison of the predictions of the two artificial neural network (ANN) training methods to experimental results showed strong alignment [15, 16]. To advance the multi-layer perceptron, a nonlinear mapping technique was used within the ANN model, the correlation values of 0.995, 0.980, 0.999, 0.985, and 0.999 were achieved with specific fuel consumption, exhaust gas temperature, thermal efficiency, hydrocarbons, NOx, and smoke emissions [17]. Then, the estimates of the engine emissions and performance was

determined utilizing ANNs model and ranged from 0.97 to 0.99 correlation coefficients with experimental data [18]. Further, the engine emissions and performance were estimated for palm biodiesel by feed-forward back propagation ANN model with given predictors and the value of correlation coefficient of determination was greater than 0.99 and mean absolute error was 1.879% [19, 20].

These form a basis for using the ANN model that predicts the engine parameters with correlation values R of 0.9994, 0.9995 and 0.9999 for training, testing and validation respectively, but with back propagation algorithm. The propagation done by the forward and backward propagation Levenberg-Marquardt algorithm, and this model had the three-layer with 10-neuron mean squared error [21]. ANN modeling resulted into R^2 values of 0.88- 0.95 with low MRE and RMSE were 3.57- 6.86 and 0.89-1.15respectively. High levels of engine performance and low levels of emissions were realised with a BSFC of 0.3 kg/kWh, BTE of 30.8 % and a peak cylinder pressure of 65.6 bar [22, 23]. But prediction accuracy was within 7% of the model's estimations, emission values were 0.0107% CO, 853 ppm NOx and 26 ppm HC [24]. The engine performance emission forecast is also done using another extreme learning machine model with a kernel based approach with average absolute percentage error that are 2.090% for Smoke O; 1.482% for BTE; 4.597% for CO; 2.224% for NOx, and 1.363% for BSFC [25].

Based on a central composite design and a response surface methodology, optimized conditions were found to be that with a load of 14.49 N·m and a 2.47% JP-8 methyl ester ratio. The outputs recorded under these parameters corresponded to a CO of 724 ppm, IMEP of 3.71 bar, NOx of 168.62 ppm, and BSFC of 193.46 g/kWh [26]. $R^2$and RMSE values close to 1 were obtained to evaluate the performance of ANN model and to test its accuracy in forecasting essential combustion parameters. R values showed reliable performance and emission predictions with modest RMSE for results. At 240° BTDC, the optimum biodiesel–diesel blend of 13% biodiesel was found to balance emissions and performance well using optimization [28]. This investigation centers on several exemplary neural network architectures. It was shown that ELM outperforms LS-SVM and RBFNN by using logarithmic transformations, and that PSO outperforms SA in allowable computation times [29]. An ELM-WT model was developed for engine performance prediction, with an correlation value exceeding 0.97 suggests near-perfect cohesion, Pearson R > 0.97, and RMS error less then 2.79 [30,31]. Notably, the most efficacious outcomes were derived from an engine fuel composition of 20.22 %, an engine rotational velocity of 1483.39 revolutions per minute, and a utilization parameter of 95.6 % load. The ensuing configuration yielded a brake thermal efficiency of 20.61%, accompanied by a brake specific fuel consumption of 0.32 kg/kWh, and a brake specific energy consumption of 6.14 MJ/kW. Notably, CO emissions comprised 0.08963% and hydrocarbon emissions amounted to 18. Concurrently, this study employed a neural network model to forecast the engine's performance and emissions as a function of engine load, biodiesel percentage, and the concentration of ZnO nano additive. This model reached convergence at 0.01528 with MSE of 0.00128 in the time of 0.00452 using hidden neurons 15. The model also proved responsiveness showing coefficients of determination higher than 98% for BTE and higher than 99% for BSFC. But the amount of CO, HC and smoke emissions declined by 8.26%, 2.08% and 3.08% respectively; On the other hand NOx and CO2 emissions raised to 22.39 % and 3.53% respectively [35,36]. Prediction of engine emissions and performance using the Complex Interactions ANN model was more accurate than that using the conventional ANN models, including the Extreme Learning Machine model.In addition, engine performance and emissions were optimized by a Taguchi approach, with ANN and multiple regression models to evaluate errors. BSFC and CO have larger deviation of 4.6%, 1.26%, 2.96% and 29.05% and NOx and HC errors are 1.26% and 2.96%, respectively, with thermal efficiency. The regression model had a standard deviation of 0.095, an adjusted R^2 of 0.972, with an accuracy of 18.482. The performance and emission metrics were highly correlated to each other using Kling Gupta efficiency (KGE) values from 0.9947 to 0.9997, indicating that the Boosted Regression Tree (BRT) model outperforms the ANN model [37].

The findings also show the effect of EGR, Biodiesel, diesel, Al2O3 nanoparticales and hydrogen on emissions and performance. HC and CO emissions were reduced by 14.9% and 11.7%, respectively, 30% biodiesel. Torque and power increased 4.89 percent while increasing diesels HC by 5.4 percent, CO by

5.8 percent, and NOx by 8 percent, adjusting for Al_2O_3 concentration from 30 ppm to 90 ppm. However, H addition resulted in 7.19% [38] increases in CO emissions. A study of previous studies gave emphasis to those studies that focused on diesel engine emissions and performance with methyl ester/diesel blends. However, by virtue of their still significantly inferior methyl ester yields, compared to used temple oil (UTO), these oils potentially fill an important, current gap in enabling the commercialization of non-edible oils as an environmentally sustainable cultivation option. Biodiesel was produced with transesterification using UTO that was combined with the diesel at a volume ratio of 25%, 50%, 75% and 100%. Thus, the resulting properties are in good agreement with ASTM standards for diesel fuel. Additionally, a novel ANN model to predict emissions as well as engine performance is introduced in this study for all UTO biodiesel-diesel blends and engine speeds so that repeated physical testing is not necessary. The engine system is represented effectively by the ANN model as it captures the complex interaction among the engine system components in the real time by dynamically adjusting the engine conditions to gain higher responsiveness and adaptability. This model also dramatically decreases time, labor, and money costs, making it a robust solution for dealing with complex, non linear data with a lesser formal exposure to statistical training. Results of the experimental data were confirmed that the ANN model effectively minimized testing and accurately predicts engine suitability for biodiesel blends. Key metrics of engine performance involve fuel-air ratio, power output, fuel efficiency, heat conversion rate, and air volume management, alongside emission metrics tracking soot, carbon monoxide, hydrocarbons, and nitrogen oxides levels.. It shows great potential in model engine behaviour under varied conditions.

2. Materials and Methods

2.1 Fuel preparation

Used temple oil (UTO) is high viscosity and cannot, due to this, be used directly in the CI engines without modification. Transesterification was used to process the oil to separate it into methyl ester and glycerin. UTO was first heated to 110°C to remove moisture and then filtered. A temperature monitored magnetic stirrer and thermometer were attached to a flask of preheated oil inside of which a flask of preheated oil was poured into a condenser. A methoxide solution was prepared by dissolving 1.5% potassium hydroxide (KOH) by weight in methanol, using a An molar ratio of 9:1 methanol to oil. The methoxide solution was vigorously mixed with heated oil at 60°C for 90 min to obtain methyl ester and glycerin. The ester and glycerin were separated after separation by allowing them to sit in a separating funnel for 24 hours. Warm water was used to remove residual catalyst, impurities and unreacted methanol. All water left in the biodiesel was removed by a rotary evaporator. Proper properties of each blend are shown in Table 1 concluding with final diesel to methyl ester blend ratios of 25, 50, 75, and 100%.

Table 1. Properties of Used Temple Oil Biodiesel

Properties	Biodiesel obtained from used temple oil	ASTM Standard for Biodiesel	Equipment utilized
Density	0.855	0.875	Hydrometer
Viscosity	3.9	1.9-6.0	Brook field viscometer
Flash point	105	100.0 min.	Pensky Marten Apparatus
Fire point	122	130	Pensky Marten Apparatus
Cloud point	9	-3 to 12	PE-7200I
Pour point	56	-10 to 12	PE-7200I
Calorific value	40129 kJ/kg	-	Bomb calorimeter
Acid value	0.52	0.80 max.	pH meter
Solubility in H2o	Insoluble	Insoluble	-

Color	Light golden	Light golden	-
Odor	Light soapy order	-	-

3. Experimental Test Ring

3.1 Engine setup

The engine undergoing examination is a single-cylinder DEUTZ F1L511 unit with a power output of 5.775 kW at a rotational speed of 1500 rpm, featuring a stroke length of 105 mm and a bore diameter of 100 mm. A compression ratio of 17.5:1 is also exhibited by this engine configuration. A nominal degree of fuel injection timing is employed, commencing from an initial injection timing of 240° before top dead centre (BTDC). A 10.5 kW Meccalte AC generator was used to simulate load conditions and coupled to the test engine. Sharp edged orifice was used through the air box to measure intake airflow; fuel flow rate was found from the burn time for 25 cm^3 of fuel. Intake and exhaust temperatures were monitored by calibrated K type thermocouples. Gaseous emissions including carbon monoxide, nitrogen oxides, and hydrocarbons were quantified utilizing a multi-component gas analyzer and smoke meter. Cylinder pressure measurements were obtained with a water-cooled piezoelectric pressure transducer, which was installed flush to minimize resonance effects and enabled real-time monitoring of pressure up to 250 bar. Piston position was detected through a proximity sensor located on the output shaft. Derived combustion parameters were calculated using pressure-crank angle graphs, which were subsequently averaged over 120 engine cycles. Data acquisition and analysis were facilitated using a software platform and a dedicated data acquisition card. Testing was carried out with the engine full load at speeds of 800 and 1800 rpm. The engine was then reheated to exhaust temperatures with pure diesel fuel, after which was tested. One time steady state conditions were reached three measurements were taken for each test to ensure accuracy. Error sources were equipment selection, ambient conditions and instrument calibration; however, error analysis was performed to validate accuracy. The three run average was used as reliability for each result.

The temperature measurement range for the thermocouples exhibited a scale spanning 0 to 1300 K, coupled with a precision of ±1 degree Celsius and an uncertainty of ±0.15. The CO2-free hydrogen indicator demonstrated an accuracy of ±10 watts, whereas the uncertainty was ±0.2 watts across the 250-7000 watt measurement spectrum. The analytical measurement ranges for exhaust components comprised: carbon monoxide concentrations between 0 and 10 percent, hydrocarbon concentrations between 0 and 20,000 parts per million, and nitric oxide concentrations between 1 and 5000 parts per million; each of these ranges exhibited an uncertainty of ±1. The maximum total experimental uncertainty was calculated based on Equation 1 to be 3.33%. WR is the uncertainty in the overall test rig, R being independent and X dependent measurement.

$$WR=\sqrt{\left(\frac{\partial R}{\partial x_1}\partial x_1\right)^2+\left(\frac{\partial R}{\partial x_2}\partial x_2\right)^2+\ldots\ldots+\left(\frac{\partial R}{\partial x_n}\partial x_n\right)^2} \quad (1)$$

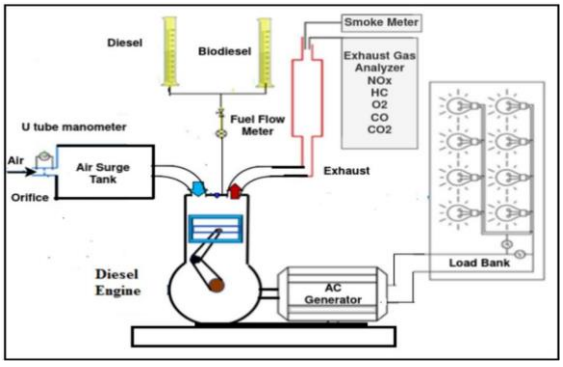

Figure 1. Schematic diagram of experimental setup.

3.2 ANN Methodology

A mathematical model is developed in this application, using a set of experimental input and output data from which a relationship is formed that enables engine performance and emission to be predicted for varying fuel and engine speeds mixture combinations, thus eliminating the need for repetition of experiments. The engine performance and emissions are predicted by this study using an artificial neural network (ANN) as a function of engine speed and biodiesel ratios. ANN plays the role of mathematical representation of the neural behavior of biological systems, including the brain [39, 40]. A single neuron, the basic unit of an ANN (in schematic form), is shown in Fig. 2.

Here Artificial Neural Network (ANN) is a suitable methodology employed to model diesel engine performance and emissions on the basis of its capacity to mimic the intricacy, complexity and non-linearity of engine dynamics and emission processes. Several interacting variables influence diesel engine emissions and performance, defining nonlinear relationships that are difficult to identify accurately using traditional regression techniques. ANNs also provide a large advantage in that they can learn and determine important features directly from data and poor quality, domain-specific feature engineering can be avoided. It is this adaptability, which enables the utilization of several input data sources, such as sensor and time series data, typical of engine monitoring systems, to be integrated. In addition, ANNs can generalize over all the domains of variable operating conditions and give reliable accuracy in real world application.

However, because engine performance and emissions are high-dimensional and noisily dependent, there are advanced computational resources and neural network frameworks used in training on these datasets. As a result, ANNs are suitable for modeling projects aimed at engine optimization, with respect to emissions, environmental regulations compliance and targets of efficiencies. Noteworthy types and architectures of ANN models in the relevant literature are reviewed, encompassing feed forward, recurrent, feedback, classification, radial basis function, sequence-to-sequence, and modular models [41-44]. This study leverages feed forward artificial neural networks, exhibiting satisfactory performance even with a solitary hidden neuron and multistage processing.

Nevertheless, the neuron is given the signal value, wi, and the relevant (weight) coefficients together with the input parameters, xi. The first estimation process requires the introduction of the weight coefficient values.

The result of the linear addition to the sum S is with the bias to be b and signal values. The minimum is set by the bias magnitude. In order for the neuron to respond the incoming information it requires a value of S.

$$S = \sum_{i=1}^{m} x_i w_i + b \qquad (2)$$

The calculated value of S is either represented by the expected value y~i of a known variable yi, or it passes through the activation function ~ and is transmitted to following neurons. Fully coupled feed-forward ANNs are taken into consideration in this work. The architecture of artificial neural networks is characterized by a synaptic connection wherein each neuron in a particular layer distributes its signals to every neuron in the subsequent layer. Typically, these networks comprise ζ total layers, where ζ − 2 hidden layers are present, and are comprised of nζ neurons. The signal magnitude, Sζij, at neuron j in the ζth layer is a function of the preceding layer with n ζ−1 neurons, calculated as per the given formula.

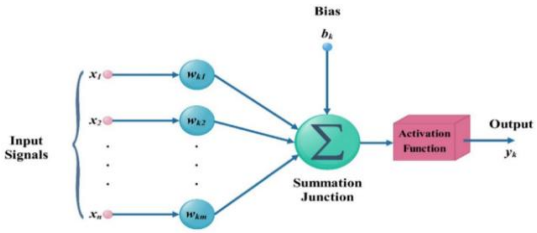

Figure 2. ANN Configuration

The rectified linear unit activation function was utilized for the hidden layers, characterized by its ability to output non-negative values, as formulated by .

$$S^{\zeta}_{ij} = \Phi\left(\sum_{i=1}^{n^{\zeta-1}} x_i w_i + b\right) \quad (3)$$

$$\Phi(S) = \max(0,X) \quad (4)$$

A linear activation function was implemented at the output layer.

$$\Phi(S) = X \quad (5)$$

Utilising equation (3), the output parameter vector is computed throughout the artificial neural network (ANN) architecture, thereby enabling the optimization of weights and biases via the training procedure to minimise predictive loss.

The dispersion between actual and predicted variable values Y comprises the discrepancy function, denoted as E, which is quantified via the mean squared error (MSE) metric employed within the existing model. Furthermore, the implementation encompasses various optimization methodologies, including adaptive sub gradient techniques, stochastic gradient descent strategies (which encompass the adaptive moment estimation algorithm, ADAM) and Nesterov momentum modifications, are implemented to alleviate loss function optimization. [40–46]. For the current model, the method was applied to speed up ANN training with ADAM. Additionally provided are the ranges at which the input parameters can be specified. For instance, the maximum engine speed is 1800 rpm, and the maximum mix ratio is 100%. The reason for this issue is that the gradient of the loss function gradients is greatly affected by the weights value , which results in a significant training time. The "Min − Max" normalization procedure was used by the current model to address the given problem [47, 48]. Therefore, the following formula was used to first normalize all of the input data:

$$X_{norm} = \frac{X - min(X)}{max(X) - min(X)} \quad (6)$$

For each input variable, normalization is performed to ensure a uniform range between 0 and 1. The cumulative impact of input variables can be determined by summing the associated weights and biases for the respective neurons at a given layer.

$$I = (n^{\zeta})^2 + \sum_{i=2}^{\zeta-1} n^i . n^{i+1} + \sum_{j=1}^{\zeta-1} n^j + n^{\zeta-1} . n^{\zeta} \quad (7)$$

It is found that the ANN prediction accuracy is influenced by more parameters when more neurons are used. However, over fitting could result from having too many neurons [41]. The datasets used for training and validation is isolated from the larger datasets. Notwithstanding instances of over prediction by the neural network, this strategy mitigates the propensity for over fitting by talkatively optimizing the loss function [41]. Within the framework of this study, the overall datasets consisted of 80% validation and 20% training.

3.3 Training ANN

This investigation utilised Artificial Neural Network (ANN) to forecast diesel engine performance and emissions, based on a specially per-determined datasets consisting of 25 discrete points, evenly dispersed throughout the input feature space. This was chosen as a uniform distribution all over input space so that there is no bias and the generalization capacity of the ANN is increased. Top to increase training efficiency and performance, the dataset was normalized. Despite the limited size of the data set, the ANN was able to learn the underlying patterns thanks to the uniform distribution and normalization, and it produced reliable and accurate predictions about the performance of diesel engines. Forward propagation is made on the input variables, loss function is calculated, then biases and weights are corrected using a

modified back propagation inference. To make sure the loss function converged, we then repeated this process for 50,000 epochs. The programme code was formulated utilizing Python 3.0, in conjunction with the Keras open source library, an integral component of the TensorFlow artificial neural network framework. The model we currently use is a multi layer perceptron, with different numbers of neurons in each layer [50–54]. At first a procedure starts to initialize the training variables like weights … (biases) with truncated normal distribution. The model finds the best number of neurons by comparing the loss function values for training and validation datasets and thus find the most influential parameters for getting the optimization on loss function. In this model there are two neurons in the input layer to represent engine speed and mix ratio.

I utilized an output layer with nine neurons and five hidden layers, each with sixteen neurons. Engine performance metrics and exhaust pollutants presently under investigation encompass air-fuel ratio, carbon monoxide, hydrocarbon emissions, carbon dioxide emissions, smoke, brake-specific torque, power output, brake-specific fuel consumption, brake thermal efficiency, and volumetric efficiency. Consequently, as shown in Fig. 3, the ANN structure is 2; 16; 16; 16; 16; 16; 16; 9. As a result, I = 1289 parameters were used, resulting in the convergence graphs shown in Figure 4 with a 1.1035% MAPE and a 5.0943 MSE, respectively.

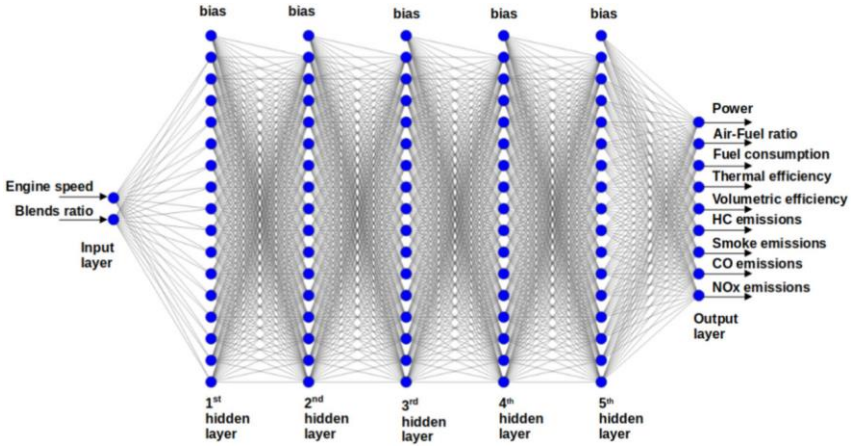

Figure 3 illustrates a visual representation of the neural network's structural framework

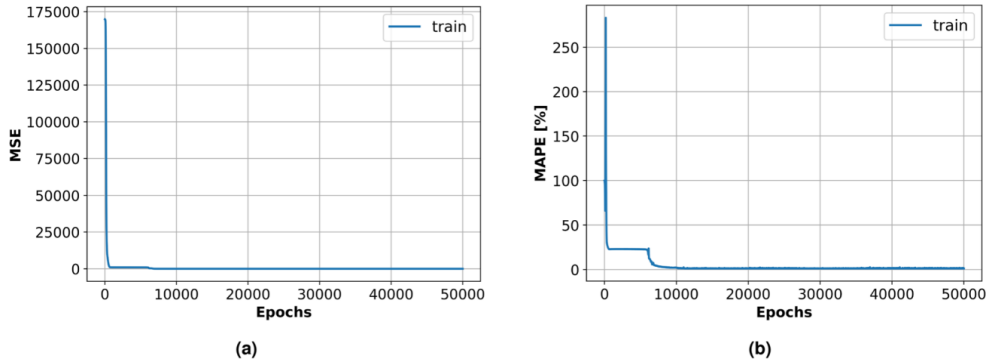

Figure 4. A visual inspection the mean squared error (MSE) and mean absolute percentage error (MAPE) metrics exhibit convergence characteristics.

An iterative procedure of alternating the comparison of the training loss on datasets was used to optimize the architecture of Artificial Neural Networks (ANN) [55]. Following the evaluation of different configurations, we found an optimal structure with 5 layers of hidden neurons, each having 16 neurons. A systematic approach was employed to vary the number of hidden layers and neurons, thereby facilitating

an evaluation of performance metrics to identify the optimal model. Optimal loss function values during training were achieved by navigating a balance between predictive efficacy and model complexity.

3.4 Accuracy of performance

As proxies for predictive efficacy, the following five evaluation metrics were employed in our analyses: Evaluative metrics provide disparate viewpoints on predictive model efficacy. Indices such as Mean Squared Error, Mean Absolute Percentage Error, and Mean Squared Logarithmic Error serve as efficacy indicators, with lower scores signifying enhanced precision. The Coefficient of Determination (R^2) and Correlation Coefficient (r) represent the degree of fit between predicted and actual values, where values approximating unity signify excellent concordance. Conversely, optimal model performance underscores the challenge of achieving error measures approaching zero; hence, models displaying near-zero error and elevated R^2 or r values are regarded as superior.

Equation 8 is purported to embody the Mean Squared Error (MSE), representing the average of squared deviations between observed values and predictive outcomes derived from a model.

$$\text{MSE} = \frac{1}{n}\sum_{i=1}^{n}(y_i - \hat{Y}_i)^2 \tag{8}$$

Where n is the number of data points, yi is the actual value $\hat{Y}_i$ is the predicted value and $(y_i - \hat{Y}_i)^2$ is the squared deviation for each prediction.

The Mean Absolute Percentage Error (MAPE) is formulated as the average of absolute discrepancies between empirical measurements and model-predicted outcomes, expressed as a percentage (Eq. 9).

$$MAPE = \frac{1}{N}\sum_{i=1}^{N}\frac{|y_i - \widehat{y_i}|}{|y_i|} * 100 \tag{9}$$

MSLE is in fact a measure of relative deviation from log transformed experimental and predicted values. In a similar manner like large deviations in the large values, MSLE also accounts for small deviations in small values, providing a good route for proportional error assessment (Equation 10).

$$MSLE = \frac{1}{N}\sum_{i=1}^{N}(log(y_i + 1) - log(\widehat{y_i} + 1))^2 \tag{10}$$

It is a statistical measure called the Coefficient of Determination, R2 which defines the proportion of variance in the predicted values that the experimental data can explain. Equation 11 defines it, meaning how well the observed data are predicted by the regression model.

$$R^2 = \frac{SSR}{SST} = \frac{\sum_{i=1}^{N}(\widehat{y_i} - \bar{y})^2}{\sum_{i=1}^{N}(y_i - \bar{y})^2} \tag{11}$$

The correlation coefficient (r) can be estimated by an effective equation that can be directly applied to ANN model predictions ($\hat{Y}_i$) and their experimental values (yi) (Equation 12).

$$r = \frac{\sum_{i=1}^{N}(y_i - \bar{y})(\widehat{y_i} - \bar{\widehat{y}})}{\sqrt{\sum_{i=1}^{N}(y_i - \bar{y})^2 \sum_{i=1}^{N}(\widehat{y_i} - \bar{\widehat{y}})^2}} \tag{12}$$

All these metrics give a clear picture of the accuracy and reliability of the models as well as their consistency and can help in a determination of the whole picture of the model efficiency.

4. Results and Discussion

4.1 Brake output power

The surface with experimental scatter, Figure 5 demonstrates the effect of a mixture on engine brake power using a surface plot displaying both experimental data and model prediction as shown in Figure 5

b and line graphs in Figure 5 a. The faster engine is capable of more RPM and the brakes have greater power. Fuel usage goes up with engine speed. With increasing the biodiesel quantity, combustion backfire is quicker than diesel oil increase and also when methyl ester calorific value lowers. Compared to pure diesel, biodiesel may result in fuel atomization and vaporization problems that stem from its greater density and viscosity as well as lead to poor air-fuel mixing. Mixtures of diesel fuel that include biodiesel take more fuel to get the same maximum power output. Pure methyl ester (B100, 0% Diesel) produces its smallest output power under full load and at exactly this engine speed by approximately 25 percent less then the diesel oil.

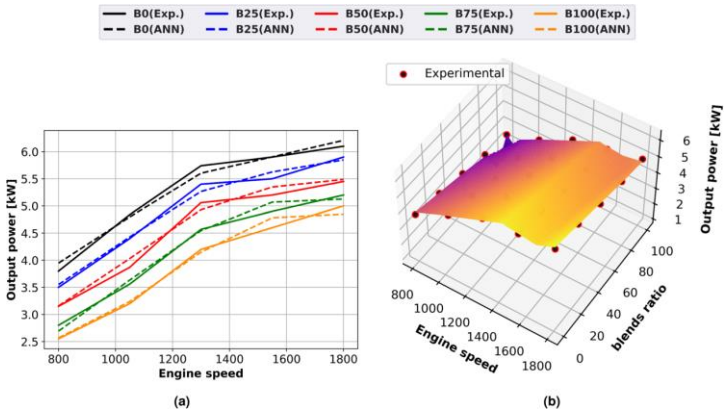

Figure 5. The output power of methyl ester blends at different engine speeds and comparison of experimental results with artificial neural network predictions. performance analysis and graphical representations of the experimental data alongside surface plots generated by the ANN model are provided.

4.2 Brake Specific Fuel Consumption

A comparison of Brake-Specific Fuel Consumption metrics is presented via graphical representations in Figure 6, illustrating both experimental and predicted trends as a function of engine speed for diesel and biodiesel blend mixtures. Notably, biodiesel exhibits elevated specific fuel consumption relative to diesel fuel across all loading conditions. This disparity is attributed to the inferior energetic efficiency of biodiesel, which necessitates increased energy input to achieve parity with diesel. The underlying causes of this phenomenon are primarily associated with enhanced viscosity, compromised combustion performance, and reduced volatility characteristics of biodiesel. The high viscosity, lack of good combustion and poor volatility responsible for the increased specific fuel consumption of biodiesel. When there was incomplete combustion caused by friction, heterogeneous mixing and atomization problems, the BSFC values for diesel oil increased. The BSFC increase when comparing biodiesel with diesel fuel was 23% at an engine speed of 1500 rpm.

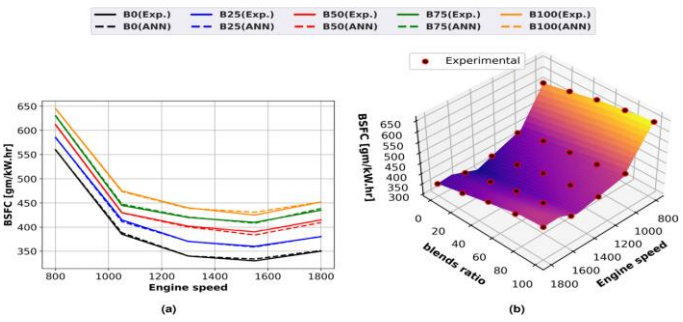

Figure 6. BSFC of biodiesel blends at different engine speeds and comparison of experimental results with artificial neural network predictions. performance analysis and graphical representations of the experimental data alongside surface plots generated by the ANN model are provided.

4.3 Brake Thermal efficiency

With experimental scatter, we improved the use of surface plots and line graphs. Fig. 7 shows the improvements in FUE and BTE over both results along with those of other experiments at diesel baseline, after treating a range of ethanol fuels up to E40 (resulting blend) levels 7a and b, respectively. Fuel consumption and rapid acceleration are at their highest in the table on the right-most 8,000 rpm unit. A diminution in thermal efficiency occurs as the concentration of methyl ester rises. Boosted thermal efficiency enhances the brake thermal efficiency ratio until the latter commences to decrease. Conversely, at low rotational speeds, augmented heat dissipation and elevated fuel consumption coexist. Additionally, at elevated speeds, exacerbated fuel consumption and frictional losses precipitate an increase in specific fuel consumption. Because bidiesel is more viscous, not as combustible, and has less volatility around diesel the thermal efficiency of it is lower. BTE decreases due to lower volatility and calorific value of biodiesel compared with diesel oil. Consumption rises and a lot of heat is lost at lower engine speeds. Methyl ester Your overall thermal when compared with diesel fuel declined by 24% at the state of work from maximum load, 1500 rpm.

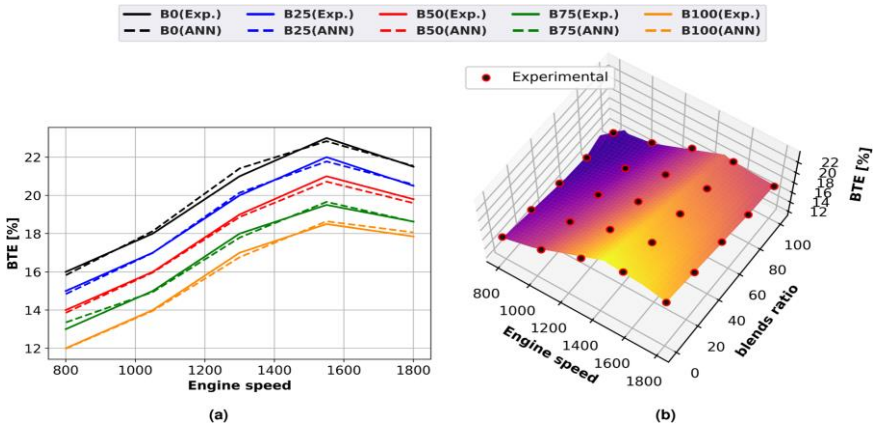

Figure 7. Thermal efficiency of biodiesel blends at different engine speeds and comparison of experimental results with artificial neural network predictions. performance analysis and graphical representations of the experimental data alongside surface plots generated by the ANN model are provided.

4.4 Air fuel ratio

Figures 8a and 8b illustrate line and surface plots delineating the relationship between engine speed and the diesel and biodiesel blends' fuel-air equivalence ratio, accompanied by experimental data corroborations. Notably, the equivalence ratio exhibits a propensity to ascend in conjunction with increased engine speed due to the concomitant augmentation in fuel flow rate necessitated. Fossil fuels oxidize and form carbon with oxidizing atom ratios that are an order of magnitude lower than those of biodiesel, which is less prone to oxidation. Biodiesel has a slower rate of consumption because its calorific value is greater, and this is why. Compared to diesel blends, biodiesel blends exhibit a more favourable air-fuel stoichiometric ratio due to their oxygen 11% enriched composition. Like diesel, biodiesel blends also have a lower stoichiometric air-fuel ratio, and the density of biodiesel blends depend on the methyl ester content (i.e., the amount of biodiesel), which increases with biodiesel proportion. When biodiesel is mixed with diesel, fuel consumption per volume increases, but decreases on the true air : fuel ratio. The equivalence ratios of the methyl ester compared with that of the pure diesel decrease by 15% in Full Load and at 1500 rpm engine speed.

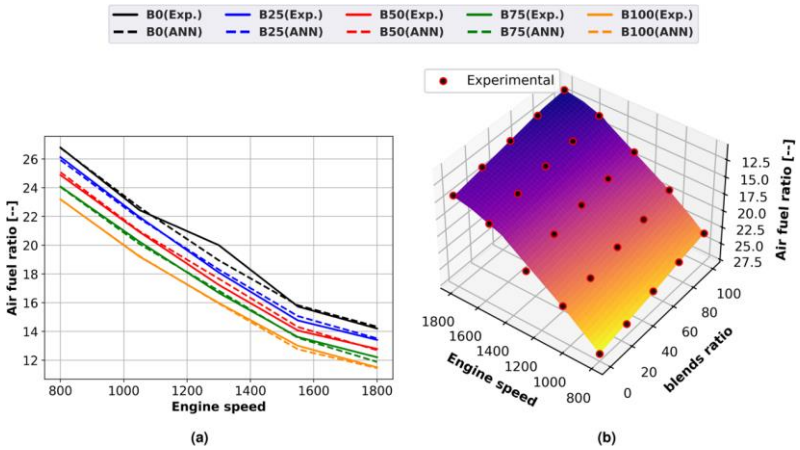

Figure 8. Air-fuel ratio methyl ester at different engine speeds and comparison of experimental results with artificial neural network predictions. performance analysis and graphical representations of the experimental data alongside surface plots generated by the ANN model are provided.

4.5 Volumetric efficiency

Line graphs and experimental scatter is used to present how volumetric efficiency changes with engine speed for expected and actual performance as diesel oil and biodiesel blend are used in Figure 9a and for surface plots in Figure 9b. Volumetric efficiency decreases as engine speed increases because as there is increased flow restriction in the intake manifold, and intake valves, and the air filter as these restrict the amount of air into the cylinder. The fact was that the volumetric efficiency of biodiesel blends with higher ethyl ester content was observed. Also, the exhaust gas temperatures of all methyl ester blends were higher than that of diesel fuel due to more complete combustion using less air that allows extra oxygen present in the methyl ester fuels mixing. Biodiesel blends have an oxygen content of 11% by weight and therefore require less air than DFL. Finally, the increase in residual gas temperature is most important to volumetric efficiency, especially with engine speed. Restrictions in the intake valve, manifold and air filter, combined with severe throttling of the air intake by the restrictions in the intake at higher engine speed reduce the amount of air admitted to the cylinder. Latent heat of vaporization and thermal properties are different for biodiesel blends of these types than for B, and lead to higher cylinder temperature and lower intake air temperature than B diesel. Comparing diesel fuel with B 100, the volumetric efficiency was 4% higher for diesel fuel than for B100.

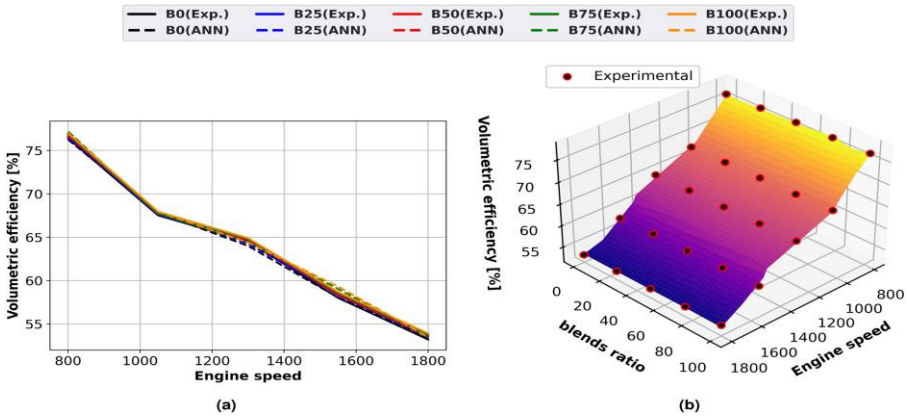

Figure 9. Volumetric efficiency of biodiesel blends at different engine speeds and comparison of experimental results with artificial neural network predictions. performance analysis and graphical representations of the experimental data alongside surface plots generated by the ANN model are provided.

4.6 CO emission

The CO emissions (Fig. 10) is engine speed dependent. In both the line graphs (Fig. 10a), and thus also in Fig. 10b, experimental scatter surface plots, CO emissions initially drop to a minimum and then increase with engine speed. At lower speeds carbon monoxide oxidation rates are slower at higher temperatures, CO being produced is more dependent on engine speed. At lower engine RPM and gas cylinder temperature, the rate of CO oxidation is reduced. Biodiesel releases more carbon dioxide than diesel fuel. That's because adding oxygen to biodiesel molecules helps burn and lowers the chance of fuel rich zones. Existing data indicates that biodiesel exhibits enhanced air-fuel mixing and combustion efficacy when compared to diesel fuel, primarily due to its comparably greater oxygen content. Furthermore, experimental results demonstrate a reduction of 12% in CO emissions when B100 is used as a substitute for diesel fuel, particularly under conditions of high engine speed and maximal braking torque.

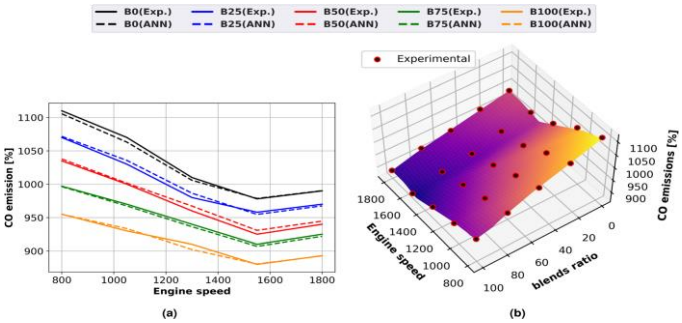

Figure 10: CO emissions from the biodiesel blends at different engine speeds and comparison of experimental results with artificial neural network predictions. performance analysis and graphical representations of the experimental data alongside surface plots generated by the ANN model are provided.

4.7 HC emission

Figure 11a depicts the correlation between HC emissions and engine speed via a line graph, while Figure 11b exhibits a surface plot displaying the aforementioned relationship in conjunction with experimental scatter plots for diesel and methyl ester, encompassing actual and ANN-predicted data. Higher HC emissions are the product of all biodiesel blends at higher engine speed, increased gasoline consumption, and hotter cylinder. On the other hand, slower engine speeds yield lower HC emissions. It's because of the very high engine load, so rich fuel mixture, and lesser presence of oxygen. Since methyl ester contains a much higher content of oxygen, therefore this reduces hydrocarbon emission regardless of the engine loads at which it is applied. Because biodiesel possesses more cetane number along with a shorter ignition delay, it emits fewer hydrocarbons compared to the same diesel fuel. For this specific application, replacing diesel fuel with biodiesel that runs at full load at 1500 rpm reduces HC emission by as much as 44 percent.

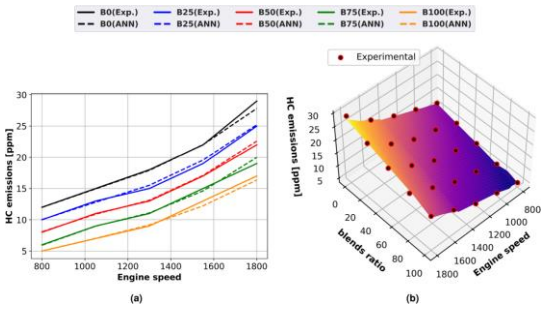

Figure 11. HC concentration of biodiesel blends at different engine speeds and comparison of experimental results with artificial neural network predictions. performance analysis and graphical representations of the experimental data alongside surface plots generated by the ANN model are provided.

4.8 NOx emission

As shown in figure 12, using actual and predicted data, engine speed affects methyl ester and NOx emissions. Figures 12(a) show line graphs and figures 12(b) surface plots with experimental data points. Such factors as cylinder temperature, residence time and oxygen content control the amount of thermal NOx produced. However, at higher speeds it becomes richer and at normal speed it is lean. The augmentation in nitrogen oxide emissions is primarily attributable to an increase in cylinder temperature. At elevated engine speeds, enhanced turbulence within the combustion chamber leads to a more affluent fuel-to-air mixture. The thermal NOx formation occurs at elevated combustion temperatures as dissociated nitrogen and oxygen react. NOx emissions increase as the proportion of methyl ester increases. The contribution of thermal NOx formation to increase the adiabatic flame temperature and to elevate NOx emissions for biodiesel over pure diesel are largely related to the cylinder temperature and oxygen content. As the turbulence increased in the engine cylinders, the air fuel mixture becomes richer and it has been known to correlate with higher thermal NOx levels. Associations between decreased air mixture uniformity, prolonged ignition latency, and increased fuel preparation times have been linked to elevated emissions. Consequently, biodiesel produced from B100, similar to diesel fuel, exhibits enhanced NOx emissions of 23% at full load operations under 1500 rpm conditions.

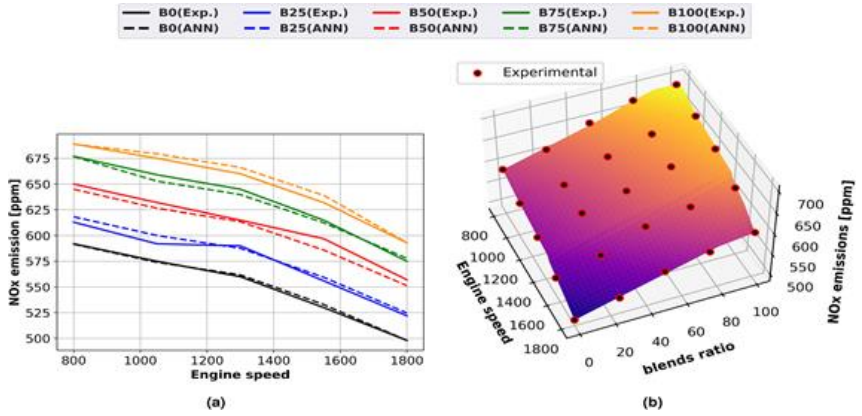

Figure 12. NOx emission for methyl ester blends at different engine speeds and comparison of experimental results with artificial neural network predictions. performance analysis and graphical representations of the experimental data alongside surface plots generated by the ANN model are provided.

4.9 Smoke emission

Figure 13: Smoke emission as influenced by line graphs of biodiesel blends and engine speed, surface plots with the experimental scatter results; projected results versus experimental results: Both projected and experimental results match. With the increase in smoke emission, the speed of the engine is also on the rise due to diesel oil, whereas there is less smoke formation since the oxygen is abundant at a lower speed of the engine. As the engine speed increases, fuel consumption increases also, reducing oxygen content and causing visual smoke emissions. On the other hand, the amount of smoke produced from methyl ester decreases with increase in biodiesel content in the fuel. Because of the biodiesel higher oxygen content, less smoke was created. As the output power and fuel consumption grow, so do the smoke emissions. The smoke formed was reduced when methyl esters were incorporated into standard diesel. Biodiesel enhances combustion and also the nature of smoke for it holds oxygen. With oxygen, biodiesel burns slowly and hence has higher particle oxidation and strength in smoke diminution when diffusive combustion is conducted. Methyl esters hold oxygen that aids in efficient ignition, reduces the emission of smoke, and boosts the combustion force. B100 biodiesel reduces the load induced smoke produced by diesel fuel by 48% at 1500 rpm under full load.

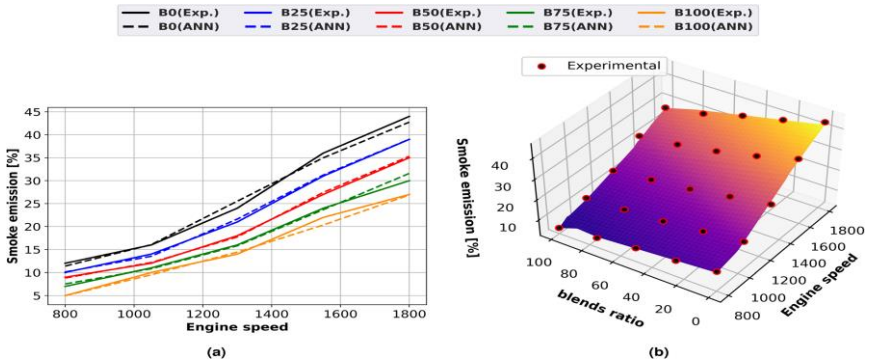

Figure 13. Smoke emission of biodiesel blends at different engine speeds and comparison of experimental results with artificial neural network predictions. performance analysis and graphical representations of the experimental data alongside surface plots generated by the ANN model are provided.

4.10 Cylinder pressure

For diesel engine operating at full load with pure diesel and various biodiesel blends as illustrated in Figure 14, the effect of crank angle on cylinder pressure. Time traces for cylinder pressure for all tested fuels were similar, and biodiesel blends had lower peak cylinder pressures than pure diesel. The faster combustion of methyl ester oils, which have higher cetane numbers than regular diesel, faster ignition and leave more fuel in the cylinder before ignition, which this reduction in pressure is due to. Analysis of ignition parameters suggests that the maximum cylinder pressure in diesel engines is attained subsequent to the culmination of ignition delay time. The combustion characteristics of biodiesel are further expedited by its inherent oxygen content, allowing for enhanced fuel droplet evaporation and ignition occurred at lighter droplet formation and mass entrainment rates. Moreover, the higher bulk modulus of biodiesel results in faster combustion and louder fuel injection system noise. The faster ignition process results in a pressure drop within the fuel circuits of biodiesel blends with diesel, which may reduce the calorific value slightly or further may impair fuel atomization. Methyl esters require less energy than diesel fuel for diffusion.Moreover, biodiesel and its blends have higher density and viscosity than diesel and thus greatly alter the spray properties, worsening atomization and vaporization difficulties. The peak cylinder pressures at full load for B0, B25, B50, B75, and B100 were 70, 68, 66, 65, and 64 bars.

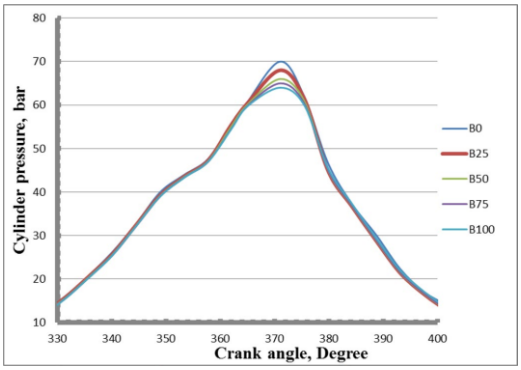

Figure 14. Biodiesel blends cylinder pressure profiles at varying crank angles.

4.11 Heat releasing rate

Under full load conditions, heat release rate analysis (HRR) patterns of diesel and biodiesel fuel blends exhibit a congruence with previously noted trends. The HRR peak rate of biodiesel blends diminishes incrementally in tandem with increasing methyl ester concentration relative to the pure diesel counterpart. This phenomenon can be attributed to the lower heat release rates during the premixed combustion phase, which is a consequence of the higher cetane number and shorter ignition delay of biodiesel. Furthermore, the lower reaction rates observed in biodiesel are also accompanied by diminished calorific values, leading to a reduced heat output. HRR and cylinder pressure decline as biodiesel proportion increases in the blend. In addition biodiesel's increased density

and viscosity affects its combustion characteristics. During the fuel-premixed phase, biodiesel blends exhibit an accelerated combustion onset by virtue of their elevated cetane number, thereby prompting a reduction in fuel consumption during the initial diffusion phase and a corresponding increase in the subsequent premixed phase. Biodiesel's inherently high cetane number presents a conundrum, as it potentially induces self-ignition at the onset of injection, thereby compromising atomization, vaporization, and fuel-air mixing. A comparative analysis of the peak heating rates (HRRs) reveals a notable trend amongst various biodiesel blends and pure diesel (B0-B100): a sequential decline from 47 Joule/CA for B0 to 42 Joule/CA for B100.

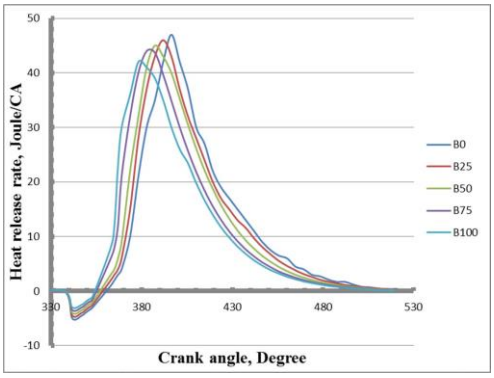

Figure 15. Biodiesel blend heat release rates for the tested fuels over the range of crank angles.

4.12 Comparison of the derived model with the experimental model

Figure 16. Performance and emission characteristics predicted by trained Artificial Neural Network (ANN) model. A plot was created to evaluate the ANN's predictions against experimental value. Along the Excellent network performance is represented by y^ =y line (with a 45° slope). The results from equations 7-15 demonstrate a high correlation with experimental and ANN-predicted values, as evidenced by the data presented in figure 16, thereby validating the predictive capabilities of this model. Fig. 16a and 16b depict the correlation coefficients (r) in the relation brake output power and brake specific fuel consumption is 0.9948, 0.9995; 16c (correlation coefficients (r) values for brake thermal efficiency): 0.998; 16d (correlation coefficients (r) values for air fuel ratio): 0.9982; 16e (correlation coefficients (r) values for volumetric efficiency): The coefficient of determination R2 values were also substantial: 0.0.999, 0.996, 0.9964, 0.9986, 0.9948, 0.9947, 0.9914, 0.9955, 9893. Also, in the MSE values, these values were low mean squared error (MSE) values were exceptionally low at 0.0109, 7.1718, 0.0331, 0.0756, 0.0886, 16.5033, 0.1861, 21.2867, and 0.5027, respectively. In all output variables, mean absolute percentage errors (MAPE) were kept under 3%, and then was 1.9455%, 0.4665%, 0.8451%, 1.0629%, 0.387%, 0.3424%, 1.7066%, 0.6049 and 2.6726%. Lastly, extremely low mean squared logarithmic error (MSLE) values: 4.0.0002, 2.2547E−05, 1.7416E−05, 0.0005, 5.7108E−05, 0.001, 3.000E−04, 9.5243E−05, 4.997E−05, and 4497E−05 were found; all of these values were below 0.002.

The ANN model's predicted performance indicators are displayed in figure 17. Performance metrics utilised for engine evaluation encompass parameters such as braking efficacy, air-fuel admixture ratio, brake- specific fuel consumption, thermal efficiency, volumetric capacity, and emissions of pollutants including hydrocarbons, particulates, carbon monoxide, and nitrogen oxides. Notably, statistical indicators comprise mean squared difference, mean absolute percentage deviation, coefficient of determination, correlation coefficient, and mean squared logarithmic difference. The efficacy of Artificial Neural Network (ANN) models is substantiated by statistically significant correlations between performance indicators, namely, higher values of correlation coefficient (r) and coefficient of determination (R^2), Subsequently, these instances are characterised by lower values for MSE, MAPE, and MSLE concomitantly. Additionally, it has been noted that the ANN model has demonstrated exceptional performance across all output parameters. For instance, in Fig. 17a, all of the correlation coefficient (r) values are greater than 0.99, A highly robust linear relationship exists between the calculated and measured values. Additionally, fig. 17b displays scores of R2 are well above 0.98 for all parameters of the output engine indicating variations in all the parameters of output ANN at more than 98 % level, and these all can be explained with that model only. MSE is described in Fig.17c. These data sets yield

minimal values of MSE = 0.0109, MSE = 0.0331, and MSE = 0.0886 for brake output power, brake thermal efficiency, and air-fuel ratio, respectively.

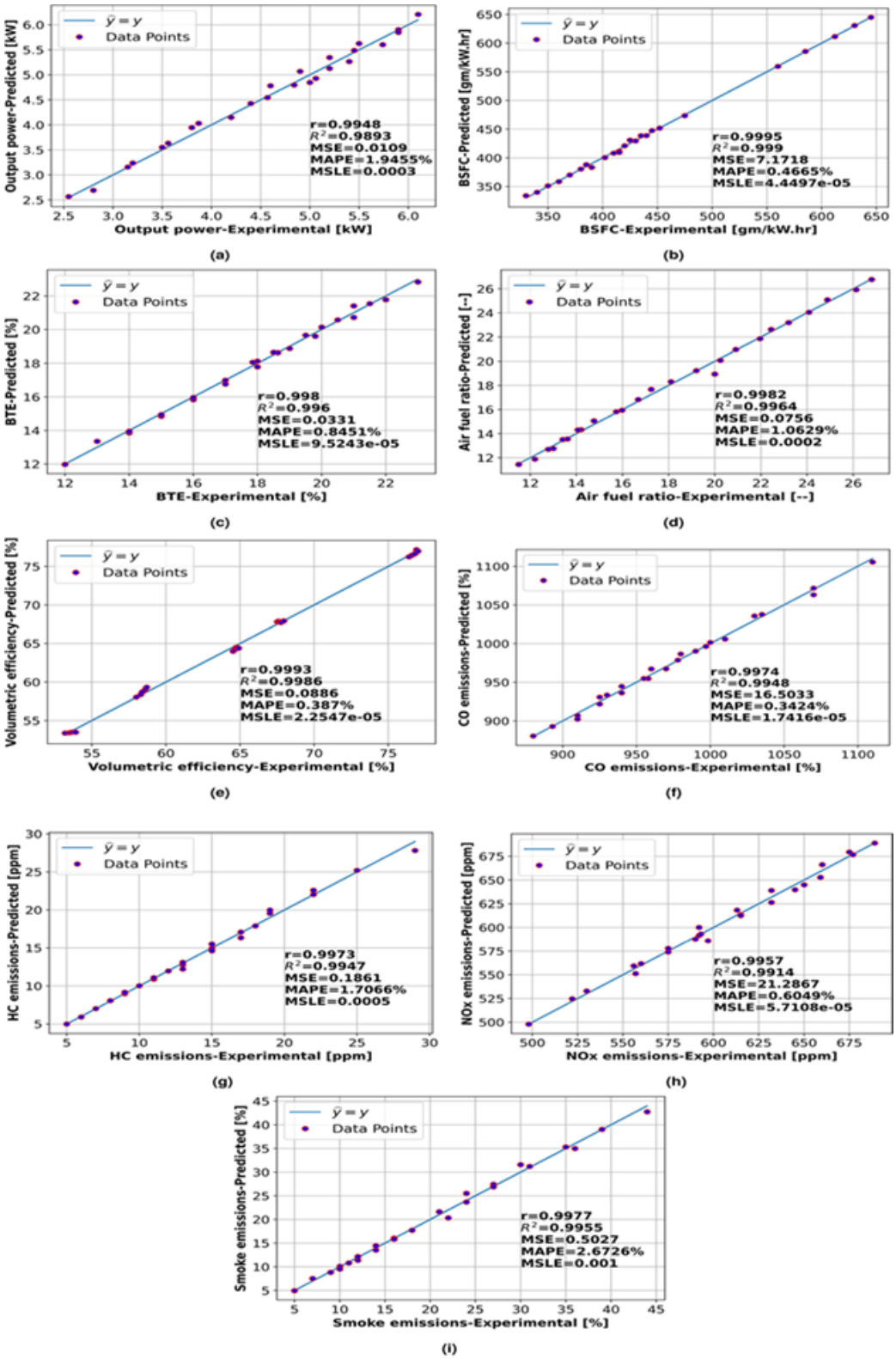

Figure 16. illustrates a regression analysis of inter relationships between key engine performance indicators and pollutant emissions, comprising brake output power, fuel consumption efficiency, thermal efficiency, air-fuel stoichiometry, volumetric efficiency, and gaseous and particulate exhaust emissions.

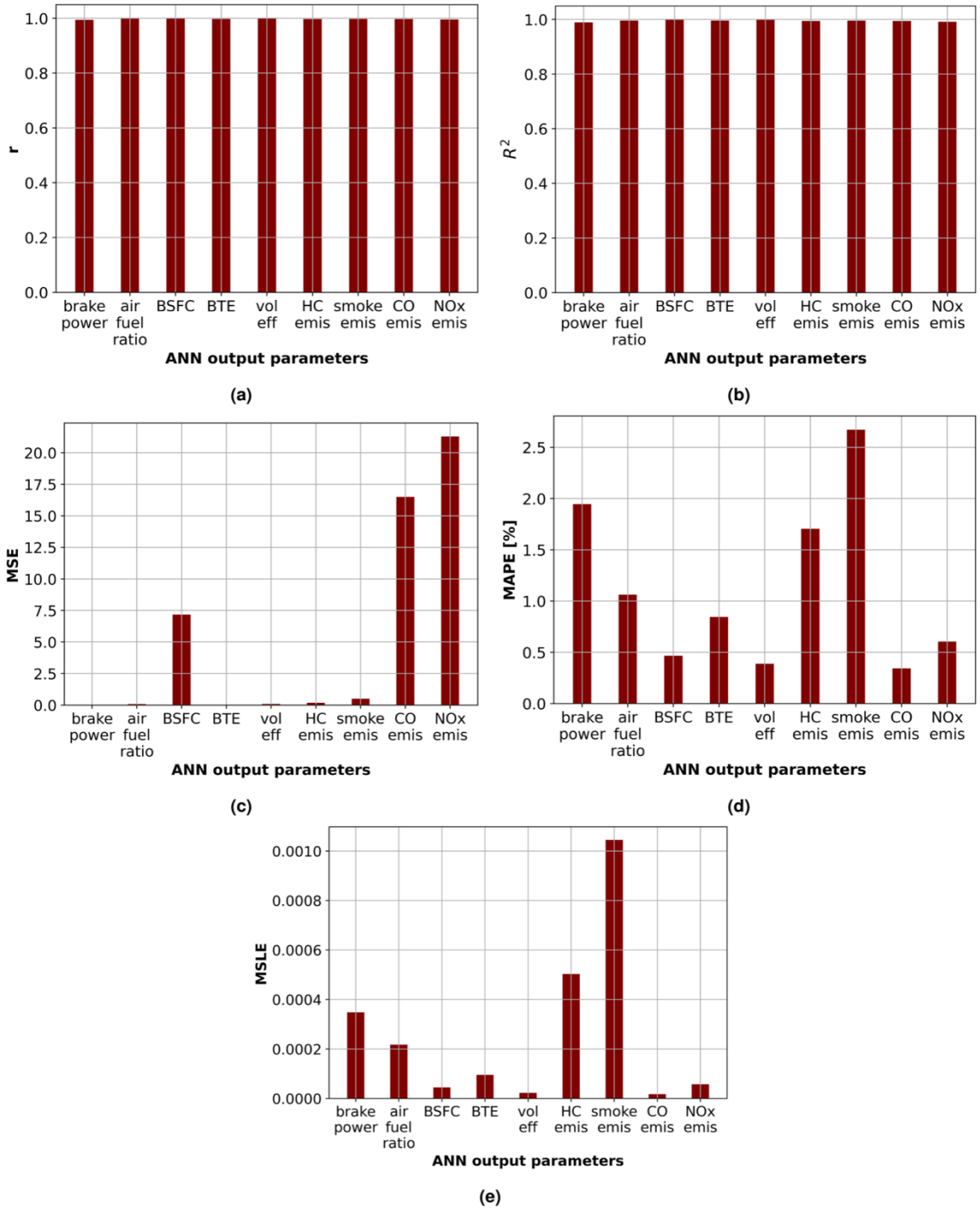

Figure 17. ANN predictive performance metrics: (a) r, (b) R2, (c) MSE, (d) MAPE and (e) MSLE.

In terms of NOx and CO emissions, this yields the highest values (MSE = 21.2867 and 16.5033, respectively). while stating the lowest value of squared discrepancies between the experimental and ANN calculated value of the aforementioned parameter. Figure 17d: The mean absolute percentage error, or MAPE, is used to display the error magnitude in percentage form. MAPE values of 0.3424% for CO emissions and 2.6726% for smoke emissions, respectively, indicate the minimum and maximum emissions. It means that the ANN on nearly reaches the best performance in predicting smoke emissions while being worst for CO emissions. The MAPE worked well (Fig. 17e) for least CO emission value although the mean squared logarithmic error (MSLE) matched it. The maximum MSLE for smoke emissions (MSLE = 0.001) was 1.7416e−05. It is a metric for the

difference between the log-transformed experimental and anticipated values. The findings show that the ANN model is highly successful in accurately predicting engine parameters.

Nonetheless, varying MSE, MAPE, and MSLE values indicate that the model reacts to various output factors. The model performed exceptionally well in predicting CO, NOx, and volumetric efficiency, however, it did not do as well when it came to smoke emissions. There are several common causes for these differences between ANN forecasts of diesel engine performance and emissions and experimental findings. First, the engine's chemical and physical processes may not be adequately represented by the ANN model. This would result in an inaccurate prediction. The majority of the time, it is caused by inadequate or biased training data that does not accurately reflect all operational settings. The model may perform poorly on new, unseen data but well on known data if it overfits the training set. Sensor measurement errors and data discrepancies during testing add noise to the ANN, hindering its generalization capability. The designed network is constrained in simplifying engine performance and emissions complexity due to its built-in assumptions. These disparities necessitate improving the models' design, complexity, and data quality, and additional representative information about conditions in the real world for better training. This may be owed to several causes; numerous connections involve the input parameters and output variables that might be complicated and nonlinear such that many interactions might have resulted in different directions with diverse magnitudes. Some may tend to be very direct, whereas for others, many can come into play. This might be due to the quality of training data impacts on the performance of ANN; however, there are some parameters for which there is complete high-quality training data. This can also be due to some intrinsic variability and noise associated with the data related to the particular outputs, as emission values are influenced by various sources outside. Additional architectural properties of the ANN, such as depth and the number of neurons used, may be more appropriate to some outputs than others. Finally, the nature through which features are extracted and transformed in the feature engineering process determines the ability of the model to predict several parameters with and without error because some feature engineering might be more representative of some outputs than others.

The ANN is a prediction tool even with small discrepancies. Results motivate further investigations into this model and find possible ways to increase it for the different output parameters. In order to develop further improvement, future investigations may consider a different design neural network or methods of data preprocessing.

Conclusions

This study investigates the direct utilisation of Used Temple oil (UTO) in diesel engines and biodiesel-diesel blends, conforming to prescribed ASTM properties. Experimental investigations involving diesel-biodiesel blends with varying proportionate compositions, namely 25%, 50%, 75% and 100%, were conducted. A model of an artificial neural network (ANN) was constructed utilizing an empirical dataset generated from experiments examining the physical and combustion characteristics of mixtures of diesel and biodiesel, thereby providing a predictive framework for performance and emissions based on rotational velocity and fuel proportions.

- Under maximum loading conditions, the power output of B100 biodiesel is observed to be significantly impaired relative to a conventionally operated diesel engine, exhibiting a reduction of 25% at a speed of 1500 rpm. This decrement in power output is accompanied by a corresponding 23% reduction in brake-specific fuel consumption. Furthermore, the thermal efficiency of B100 biodiesel is compromised, manifesting a diminution of 24% at identical operating conditions. Notwithstanding these thermal inefficiencies, B100 biodiesel is characterized by an air-fuel ratio and volumetric efficiency that are 15% and 4% lower, respectively, as compared to diesel at the aforementioned speed.

- In comparative trials with diesel fuel, utilisation of B100 biodiesel realised a statistically significant reduction in CO emissions of 12%, a decrease of 44% in hydrocarbon emissions, and an attendant 48% decline in particulate emissions when engine speed reached 1500 rpm and during maximum braking conditions. This was, however, very different from B100 at maximum load (1500 rpm) and 50% load where NOx emissions were 23% higher compared to diesel.

- The maximum HRR for B0, B25, B50, B75, and B100 was 47, 46, 45, 44, and 42 Joule/CA, respectively, while the peak full-load cylinder pressures, as indicated below, were 70, 68, 66, 65, and 64 bar.

- The ANN model exhibits outstanding prediction power across all engine output parameters. The fact that all of the parameters' r values stayed above 0.99, their R2 level values were all above 0.98, and the MSE, MAPE, and MSLE values were significantly lower suggests that the ANN model was highly predictive.

- The mean squared error of the brake torque output, air-fuel efficiency, and volumetric efficiency all drop to their lowest levels.

CO and NOx emissions showed their peak values on the highest brake thermal efficiency and equivalence ratios respectively, CO emissions had both the lowest mean absolute percentage error (MAPE) and mean squared logarithmic error (MSLE), while smoke emissions had the highest MSLE. In fact, pure biodiesel also had greater density and viscosity than diesel fuel. This results in problems with vaporization and atomization, which in turn causes the filter to block in cold weather and the fuel injector to clog. Biodiesel takes more fuel, generates less power, and loses thermal efficiency because it has a lower calorific value than diesel oil. Because biodiesel has a greater flash point than pure diesel, it may be handled and stored safely. Biodiesel's higher oxygen content improves combustion efficiency, which lowers CO and HC emissions. Diesel oil emits less NOx than biodiesel; recirculation of exhaust gases helps reduce NOx emissions. Used temple oil biodiesel containing 20% of this substance is recommended as a diesel engine substitute due to its chemically and physically analogous properties to those of diesel oil.

References

[1] Venkanna, B., Reddy, C. V. & Wadawadagi, S. B. (2009). Performance, emission and combustion characteristics of direct injection diesel engine running on rice bran oil/diesel fuel blend. Diesel Engine 14, 15.
[2] Nwafor, O. (2004). Emission characteristics of diesel engine running on vegetable oil with elevated fuel inlet temperature. Biomass Bioenerg. 27, 507–511.
[3] Huang, G., Chen, F., Wei, D., Zhang, X. & Chen, G. (2018). Biodiesel production by microalgal biotechnology. Renew. Energy 3, 378–395.
[4] Leung, D. Y., Wu, X. & Leung, M. K. H. (2010). A review on biodiesel production using catalyzed transesterifcation. Appl. Energy 87, 1083–1095.
[5] Jayed, M., Masjuki, H. H., Saidur, R., Kalam, M. & Jahirul, M. I. (2009). Environmental aspects and challenges of oilseed produced biodiesel in Southeast Asia. Renew. Sustain. Energy Rev. 13, 2452–2462.
[6] Lin, L., Cunshan, Z., Vittayapadung, S., Xiangqian, S. & Mingdong, D. (2011). Opportunities and challenges for biodiesel fuel. Appl. Energy 88, 1020–1031.
[7] Abedin, M. et al. (2013). Energy balance of internal combustion engines using alternative fuels. Renew. Sustain. Energy Rev. 26, 20–33
[8] Lee, H., Taufq-Yap, Y., Hussein, M. & Yunus, R. (2013). Transesterifcation of jatropha oil with methanol over Mg-Zn mixed metal oxide catalysts. Energy 49, 12–18.
[9] Mofjur, M., Atabani, A., Masjuki, H. A., Kalam, M. & Masum, B. (2013). A study on the efects of promising edible and non-edible biodiesel feedstocks on engine performance and emissions production: A comparative evaluation. Renew. Sustain. Energy Rev. 23, 391–404.
[10] Jain, S. & Sharma, M. P. (2011). Oxidation stability of blends of jatropha biodiesel with diesel. Fuel 90, 3014–3020.
[11] Szybist, J. P., Song, J., Alam, M. & Boehman, A. L. (2007). Biodiesel combustion, emissions and emission control. Fuel Process. Technol. 88, 679–691.
[12] Knothe, G. (2005). Dependence of biodiesel fuel properties on the structure of fatty acid alkyl esters. Fuel Process. Technol. 86, 1059–1070.
[13] Canakci, M. & Van Gerpen, J. H. (2003). Comparison of engine performance and emissions for petroleum diesel fuel, yellow grease biodiesel, and soybean oil biodiesel. Trans. ASAE 46, 937.

[14] Prasad, T. H., Reddy, K. H. C. & Rao, M. M. (2010). Performance and exhaust emissions analysis of a diesel engine using methyl esters of fsh oil with artifcial neural network aid. Int. J. Eng. Technol. 2, 23.
[15] Raghuvaran, S., Ashok, B., Veluchamy, B. & Ganesh, N. (2021). Evaluation of performance and exhaust emission of ci diesel engine fuel with palm oil biodiesel using an artifcial neural network. Mater. Today Proc. 37, 1107–1111.
[16] Castresana, J., Gabina, G., Martin, L. & Uriondo, Z. (2021). Comparative performance and emissions assessments of a single-cylinder diesel engine using artifcial neural network and thermodynamic simulation. Appl. Term. Eng. 185, 116343.
[17] Rao, K. P., Babu, T. V., Anuradha, G. & Rao, B. A. (2017). IDI diesel engine performance and exhaust emission analysis using biodiesel with an artifcial neural network (ANN). Egypt. J. Pet. 26, 593–600.
[18] Hosamani, B., Ali, S. A. & Katti, V. (2021). Assessment of performance and exhaust emission quality of diferent compression ratio engine using two biodiesel mixture: Artifcial neural network approach. Alex. Eng. J. 60, 837–844.
[19] Kumar, A. N. et al. (2020). Decanol proportional efect prediction model as additive in palm biodiesel using ANN and RSM technique for diesel engine. Energy 213, 119072.
[20] Bhowmik, S., Paul, A., Panua, R., Ghosh, S. K. & Debroy, D. (2018). Performance-exhaust emission prediction of diesosenol fueled diesel engine: An ANN coupled MORSM based optimization. Energy 153, 212–222.
[21] Hosseini, S. H., Taghizadeh-Alisaraei, A., Ghobadian, B. & Abbaszadeh-Mayvan, A. (2020). Artifcial neural network modeling of performance, emission, and vibration of a ci engine using alumina nano-catalyst added to diesel-biodiesel blends. Renew. Energy 149, 951–961.
[22] Işcan, B. (2020). Ann modeling for justifcation of thermodynamic analysis of experimental applications on combustion parameters of a diesel engine using diesel and safower biodiesel fuels. Fuel 279, 118391.
[23] Uslu, S. (2020). Optimization of diesel engine operating parameters fueled with palm oil-diesel blend: Comparative evaluation between response surface methodology (RSM) and artifcial neural network (ANN). Fuel 276, 117990.
[24] Shirneshan, A., Samani, B. H. & Ghobadian, B. (2016). Optimization of biodiesel percentage in fuel mixture and engine operating conditions for diesel engine performance and emission characteristics by artifcial bees colony algorithm. Fuel 184, 518–526.
[25] Ramachander, J., Gugulothu, S., Sastry, G., Panda, J. K. & Surya, M. S. (2021). Performance and emission predictions of a CRDI engine powered with diesel fuel: A combined study of injection parameters variation and Box-Behnken response surface methodology based optimization. Fuel 290, 120069.
[26] Simsek, S., Uslu, S. & Simsek, H. (2022). Proportional impact prediction model of animal waste fat-derived biodiesel by ANN and RSM technique for diesel engine. Energy 239, 122389.
[27] Bitire, S. O. & Jen, T.-C. (2022). The impact of process parameters on the responses of a diesel engine running on biodiesel-diesel blend: An optimization study. Egypt. J. Pet. 31, 11–19.
[28] Ardebili, S. M. S., Kocakulak, T., Aytav, E. & Calam, A. (2022). Investigation of the efect of JP-8 fuel and biodiesel fuel mixture on engine performance and emissions by experimental and statistical methods. Energy 254, 124155.
[29] Manimaran, R., Mohanraj, T., Venkatesan, M., Ganesan, R. & Balasubramanian, D. A (2022). computational technique for prediction and optimization of VCR engine performance and emission parameters fuelled with trichosanthes cucumerina biodiesel using RSM with desirability function approach. Energy 254, 124293.
[30] Kumar, S. & Pal, A. (2022). Multi-objective-parametric optimization of diesel engine powered with fuel additive 2-ethylhexyl nitrate-algal biodiesel. Sustain. Energy Technol. Assess. 53, 102518.
[31] Can, Ö., Baklacioglu, T., Özturk, E. & Turan, O. (2022). Artifcial neural networks modeling of combustion parameters for a diesel engine fueled with biodiesel fuel. Energy 247, 123473.
[32] Esonye, C., Onukwuli, O. D., Ofoefule, A. U. & Ogah, E. O. (2019). Multi-input multi-output (MIMO) ANN and Nelder-Mead's simplex based modeling of engine performance and combustion emission characteristics of biodiesel-diesel blend in CI diesel engine. Appl. Term. Eng. 151, 100–114.

[33] Shivaranjini, A Srinivasan, Anjappa SB, R Vasanth Selvakumar, E Purushotham. (2024). An Evaluation of the CNN-LSTM Model's Efficacy in Sentiment Analysis Using the Bert and Attendance Mechanisms. International Research Journal of Multidisciplinary Scope (IRJMS). Volume: 5 Issue: 2 Pages: 822-829.

[34] Pai, P. S. et al. (2011). Artifcial neural network based prediction of performance and emission characteristics of a variable compression ratio ci engine using wco as a biodiesel at diferent injection timings. Appl. Energy 88, 2344–2354.

[35] R. Jayakarthik, A. Srinivasan, S. Goswami, Shivaranjini and M. R, (2022) "Fall Detection Scheme based on Deep Learning Model for High-Quality Life," 3rd International Conference on Electronics and Sustainable Communication Systems (ICESC), Coimbatore, India, pp. 1582-1588, doi: 10.1109/ICESC54411.2022.9885675.

[36] Anjappa, S, & Ramesha, D. (2024). Experimental Investigation of the Effects of a Reduced Exhaust Gas Re-circulation Rate on the Performance and Emissions of CI Engines Running on Biodiesel made from Dairy Waste Scum Oil. Journal of Research and Applications in Mechanical Engineering. 13(1).